Applied Physics Letters

Spin–orbit torque driven multi-level switching in He^+ irradiated W–CoFeB–MgO Hall bars with perpendicular anisotropy

Cite as: Appl. Phys. Lett. **116**, 242401 (2020); https://doi.org/10.1063/5.0010679
Submitted: 14 April 2020 . Accepted: 29 May 2020 . Published Online: 15 June 2020

Xiaoxuan Zhao, Yang Liu, Daoqian Zhu, Mamour Sall, Xueying Zhang, Helin Ma, Jürgen Langer, Berthold Ocker, Samridh Jaiswal, Gerhard Jakob, Mathias Kläui, Weisheng Zhao, and Dafiné Ravelosona

© 2020 Author(s).

Spin–orbit torque driven multi-level switching in He^+ irradiated W–CoFeB–MgO Hall bars with perpendicular anisotropy

Cite as: Appl. Phys. Lett. **116**, 242401 (2020); doi: 10.1063/5.0010679
Submitted: 14 April 2020 · Accepted: 29 May 2020 ·
Published Online: 15 June 2020

View Online

Export Citation

CrossMark

Xiaoxuan Zhao,[1,2] Yang Liu,[1] Daoqian Zhu,[1] Mamour Sall,[2,3] Xueying Zhang,[1,4,5] Helin Ma,[1] Jürgen Langer,[6] Berthold Ocker,[6] Samridh Jaiswal,[6,7] Gerhard Jakob,[7] Mathias Kläui,[7] Weisheng Zhao,[1,4,a)] and Dafiné Ravelosona[2,3]

AFFILIATIONS

[1]Fert Beijing Institute, School of Microelectronics, Beijing Advanced Innovation Center for Big Data and Brain Computing, Beihang University, 100191 Beijing, China
[2]Centre de Nanosciences et de Nanotechnologies, CNRS, Université Paris-Saclay, 10 Boulevard Thomas Gobert, 91120 Palaiseau, France
[3]Spin-Ion Technologies, 10 Boulevard Thomas Gobert, 91120 Palaiseau, France
[4]Beihang-Goertek Joint Microelectronics Institute, Qingdao Research Institute, Beihang University, 266000 Qingdao, China
[5]Truth Instrument Co. Ltd., 266000 Qingdao, China
[6]Singulus Technology AG, Hanauer Landstrasse 103, 63796 Kahl am Main, Germany
[7]Institute of Physics, Johannes Gutenberg University Mainz, 55099 Mainz, Germany

[a)]Author to whom correspondence should be addressed: weisheng.zhao@buaa.edu.cn

ABSTRACT

We have investigated the spin–orbit torque-driven magnetization switching in W/CoFeB/MgO Hall bars with perpendicular magnetic anisotropy. He^+ ion irradiation through a mask has been used to reduce locally the effective perpendicular anisotropy at a Hall cross. Anomalous Hall effect measurements combined with Kerr microscopy indicate that the switching process is dominated by domain wall (DW) nucleation in the irradiated region followed by rapid domain propagation at a current density as low as 0.8 MA/cm^2 with an assisting in-plane magnetic field. Thanks to the implemented strong pinning of the DW at the transition between the irradiated and the non-irradiated region, an intermediate Hall resistance state is induced, which is further verified by finite element simulations. Such a method to control electrically multi-level resistances using He^+ ion irradiation shows great potential in realizing neuromorphic and memristor devices.

Published under license by AIP Publishing. https://doi.org/10.1063/5.0010679

Spin–orbit torque (SOT)-induced magnetic switching has attracted extensive interest due to its potential high efficiency in terms of switching time and power consumption.[1–9] Whereas single domain switching is highly desirable for SOT magnetic random access memory (SOT-MRAM) devices, domain wall (DW) nucleation followed by DW propagation has been revealed to be the dominant switching mechanism in several types of structures, including antiferromagnetic (AFM)/ferromagnetic (FM) systems and heavy metal (HM)/FM systems.[2,3,7,8] In parallel, chiral domain wall motion driven by SOT in nanowires in the presence of Dzyaloshinskii–Moriya interaction (DMI) at interfaces between HM and FM layers has shown great potential for applications in racetrack memory devices.[10–14] One potential advantage of DW driven switching is that multi-level states can be obtained by controlling the position of the DW across a nanostructure such as wires or dots. As such, domain wall memristors[15–17] and the possibility to use DW motion as synapses[18,19] have been recently demonstrated. To fully realize such promising applications, well-separated DW states should be tailored and addressed by a low current density. Recently, multi-level switching has been demonstrated in Ta/CoFeB/MgO structures assisted by an in-plane magnetic field with different magnitudes.[7] Intermediate switching can be stably reproduced without initialization in their experiments, which makes their scheme attractive. However, the necessity of varying the in-plane magnetic field hinders the practical application of this method. In this study, we demonstrate SOT-driven multi-level Hall

resistances in W/CoFeB/MgO-based Hall bars by reducing laterally the perpendicular magnetic anisotropy through He^+ ion irradiation, which is an effective method to modify the properties of magnetic multilayers.[20,21] These multi-level Hall resistances are observed at low current densities under a fixed in-plane field.

The structure of the investigated samples is W (4 nm)/$Co_{20}Fe_{60}B_{20}$ (0.6 nm)/MgO (2 nm)/Ta (3 nm), grown on top of oxidized silicon substrates using a magnetron sputtering system. The sample was then annealed at 400 °C for 2 h, leading to a crystallized phase with strong perpendicular magnetic anisotropy. The saturation magnetization and anisotropy field measurements were performed at room temperature by using superconducting quantum interference device (SQUID) magnetometry under perpendicular and in-plane magnetic fields, respectively. The films were then patterned into Hall bars consisting of 20 μm wide and 140 μm long wires including two Hall crosses with a width of 5 μm. Ti (20 nm)/Au (80 nm) current and voltage electrodes were then deposited by electron beam evaporation using a liftoff process. Then, 2 μm thick positive photoresist was spin-coated on the wafer. A lithographic mask was fabricated by direct writing using a laser lithography system. A 20 μm × 30 μm rectangular open area was designed on top of the left Hall cross, as shown in Figs. 1(a) and 1(b).

As shown in previous studies, light He^+ ion irradiation-induced interface intermixing can be used to finely tune M_s, interface anisotropy, and DMI in CoFeB–MgO structures.[18,19] Using the same ion beam parameters, the samples were subsequently irradiated through the mask by He^+ ions with an energy of 15 keV at an irradiation dose (ID) of 1×10^{19} ions/m^2. After irradiation, the photoresist was removed for further measurements. Non-irradiated and fully irradiated Hall bars were also measured for comparison.

The hysteresis loops measured under perpendicular magnetic fields for non-irradiated and fully irradiated films are shown in Fig. 1(c).

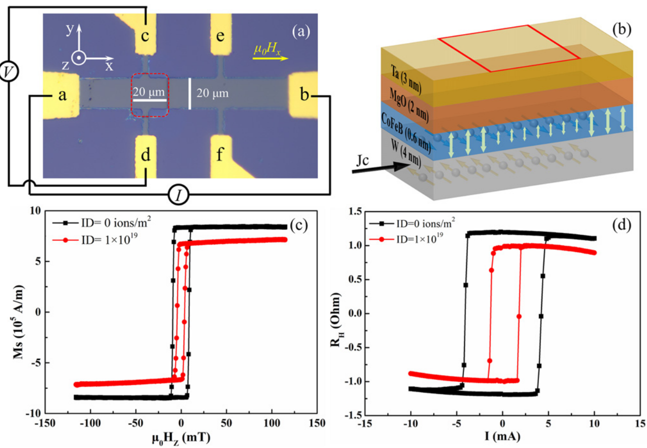

FIG. 1. (a) Hall bar structure where a–b and c–d correspond to the current and voltage electrodes, respectively. The red rectangle corresponds to the irradiated area. (b) Schematic of the W (4 nm)/CoFeB (0.6 nm)/MgO (2 nm)/Ta (3 nm) film stack. The region delineated by the red rectangle is the irradiated region of (a). (c) Hysteresis loops measured by SQUID for non-irradiated (black squares) and irradiated (ID = 1×10^{19} ions/m^2) (red dots) full films. (d) Anomalous Hall resistance as a function of applied current for non-irradiated (black squares) and fully irradiated (ID = 1×10^{19} ions/m^2) (red dots) Hall bars. μ_0H_x = 50 mT is used to assist the magnetization switching as indicated in (a).

The reduction of saturation magnetization M_s upon irradiation, about 20%, is attributed to the atom intermixing at the W–CoFeB interface.[18] In addition, we found a decrease in the coercivity H_c, which is due to the decrease in the effective anisotropy K_{eff} from 3.8×10^5 J/m^3 to 3×10^5 J/m^3 in the irradiated samples.[22] Here, K_{eff} is calculated by $1/2\mu_0 M_s H_k$, with H_k denoting the anisotropy field. Anomalous Hall resistance as a function of the SOT current is shown in Fig. 1(d) for fully irradiated and non-irradiated Hall bars. SOT switching has been obtained using a longitudinal in-plane magnetic field μ_0H_x of 50 mT. The reduction of K_{eff} by 20% (as shown in Fig. S1) under ion irradiation is accompanied by a large reduction of the switching current from 3.74 mA (4.07 MA/cm^2) to 1.55 mA (1.68 MA/cm^2), which is determined by the threshold current to induce DW nucleation as checked by Kerr microscopy. The amplitude of the anomalous Hall effect (AHE) is also decreased (ΔR = 2.4 and 2.0 Ω, for the non-irradiated and irradiated Hall bars, respectively), which is further verified by AHE measurements under perpendicular fields. The reduction rate of ΔR is about 20%, indicating that it is mainly caused by the reduction of M_s.

Next, we discuss the SOT switching in Hall bars where only one Hall cross has been irradiated [Figs. 1(a) and 1(b)]. As shown in

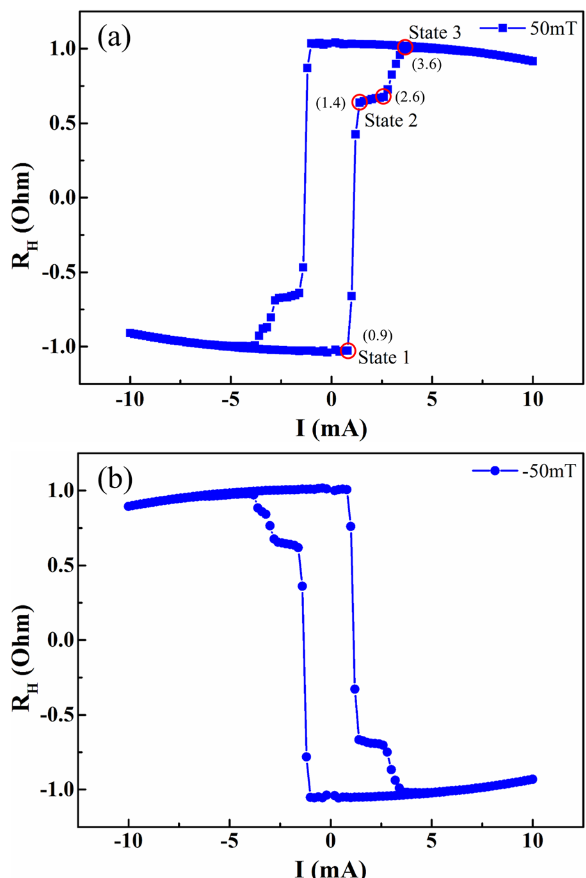

FIG. 2. SOT switching curves for an irradiated Hall cross measured under in-plane fields μ_0H_x of (a) 50 mT and (b) −50 mT. States 1, 2, and 3 correspond to down magnetization, intermediate state, and up magnetization, respectively. Numbers in parentheses in (a) refer to the current value for each point.

Published under license by AIP Publishing

Figs. 2(a) and 2(b), Hall resistance (R_H) vs current (I) curves were obtained by sweeping the DC (step 0.02 mA) under $\mu_0 H_x = 50$ mT and -50 mT, respectively. The fact that the two hysteresis loops are reversed upon reversing the direction of the in-plane magnetic field is consistent with SOT-induced switching.[1,6] The total variation of the Hall resistance $\Delta R = 2.0\ \Omega$ is close to the one obtained for the fully irradiated Hall bars [Fig. 1(d)]. The most striking result here is the presence of an intermediate state between the two saturated states.

More precisely, as indicated in Fig. 2(a), when sweeping the current from -10 mA to $+10$ mA, we observe three different states, $R_H = -1\ \Omega$ for $I_{S1} \leq 0.90$ mA (state 1), $0.64\ \Omega < R_H < 0.67\ \Omega$ for $1.40\ \text{mA} < I_{S2} < 2.60$ mA (state 2), and $R_H = 1\ \Omega$ for $I_{S3} \geq 3.60$ mA (state 3). To gain deeper insight into the process of SOT-driven intermediate state switching, we have performed further measurements using a polar Kerr microscope with electrical probes.

As seen in Fig. 3(ii), after nucleation of a reversed domain at $I = 0.74$ mA (0.80 MA/cm^2), the irradiated region is fully reversed by rapid DW propagation upon increasing the current up to $I = 1.38$ mA [1.50 MA/cm^2, see (iii) in Fig. 3]. The fact that the current density is even lower than that in the fully irradiated wire (1.68 MA/cm^2) is ascribed to the presence of an over irradiated region at the transition between the non-irradiated and irradiated areas due to ions escaping from the mask edges. When the current is further increased, the DW remains pinned at the boundary between the irradiated and non-irradiated areas because of the presence of the anisotropy gradient[23,24] induced by the He^+ irradiation. When the current increases up to 2.40 mA, a new reversed domain emerges from the right edge of the wire and propagates toward the irradiated area. The DW propagates along the electron flow, consistent with the positive sign of DMI in W/CoFeB/MgO structures[18] and the negative spin Hall angle of W.[25–27] When the current reaches 3.10 mA [see (v) in Fig. 3], the right region is fully reversed, while a new reversed domain that is probably unpinned at the irradiated-non-irradiated frontier propagates along the electron flow toward the left side of the wire. Increasing the current up to 3.58 mA, the full wire has reversed its magnetization, as seen in Fig. 3(vi).

The magnetization reversal process revealed by the Kerr microscopy images indicates that the different magnetic states shown in Fig. 3 can be correlated with those revealed by the SOT switching loop measured by AHE in Fig. 2. In particular, for the first stage indicated in Fig. 2(a) (from state 1 to state 2), the sharp reversal induced by the current at $I_{S1} = 0.90$ mA corresponds approximately to the domain nucleation[28] seen in Fig. 3(ii) at $I = 0.74$ mA. The intermediate state observed in Fig. 2 between $I = 0.90$ mA and $I = 2.60$ mA corresponds to the strong DW pinning seen in Figs. 3(iii) and 3(iv). Finally, the final reversal of the right and left side of the Hall bar [see (iv)–(vi) in Fig. 3] at $I = 2.40$–3.58 mA corresponds to the currents $I = 2.60$–3.60 mA going from state 2 to state 3 in Fig. 2.

The fact that the hysteresis loop measured by AHE and the Kerr images show a close correspondence indicates that the Hall voltage wire (width of $w_{voltage} = 5\ \mu$m wide) is sensitive to the magnetization reversal of the wire outside the wide irradiated region ($20\ \mu\text{m} \times 30\ \mu$m). In order to verify this hypothesis, we have measured Hall bars with different wire widths ($w = 20$, 10, and 6 μm) and anomalous Hall voltage probe widths ($w_{\text{voltage}} = 5$, 3, and 3 μm, respectively). We have patterned the same irradiated region ($20\ \mu\text{m} \times 30\ \mu$m) centered on the left Hall cross. Figure 4(a) shows the switching loops as a function of the wire width, indicating that the intermediate states corresponding to DW pinning at the edges of the irradiated area can only be evidently seen by the largest wires.

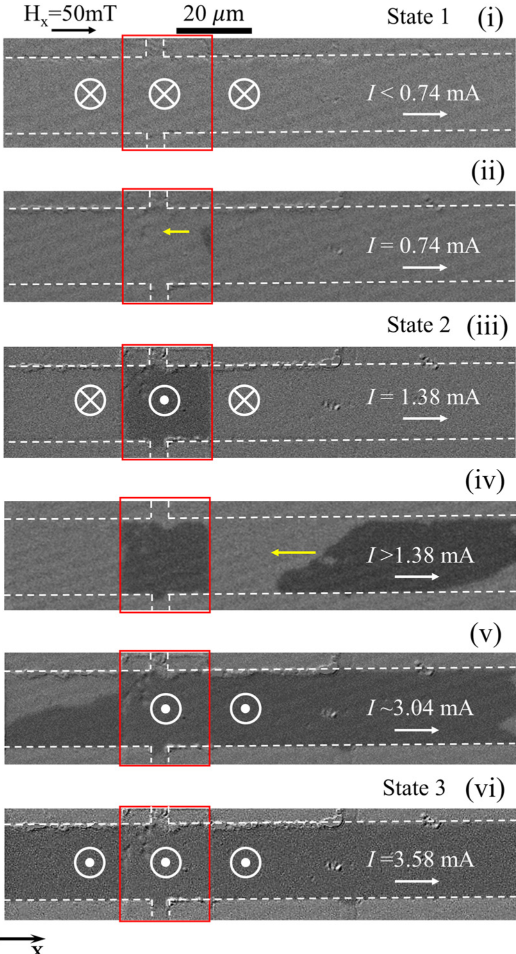

FIG. 3. Kerr images showing the SOT-induced magnetization switching process of the Hall bar for an increasing current with $\mu_0 H_x = 50$ mT. The white dashed lines indicate the longitudinal current wire and the transverse voltage wire. The red box corresponds to the irradiated area. The yellow arrows in (ii) and (iv) show the direction of domain wall motion.

This result was further verified by finite element simulations of AHE (see the supplementary material).[29] Figure 4(b) shows the schematic of the simulated cross-shaped Hall device, where the ferromagnetic materials and gold electrodes are indicated by gray and orange regions, respectively. The width of the wire w and the voltage probes w_{voltage} and the thickness of the FM layer are adopted from experimental parameters. The irradiated region with a width of 20 μm is marked by the dashed lines. We first assumed that the initial magnetization is along the $+z$ direction and then calculated the AHE resistance with a DW moving from $-30\ \mu$m to 30 μm in the Hall device. Figure 4(c) shows the normalized R_H with the DW stopping at different positions. The AHE resistance reduces sharply when the DW moves from $-10\ \mu$m to 10 μm, i.e., the magnetization of the irradiated region

Published under license by AIP Publishing

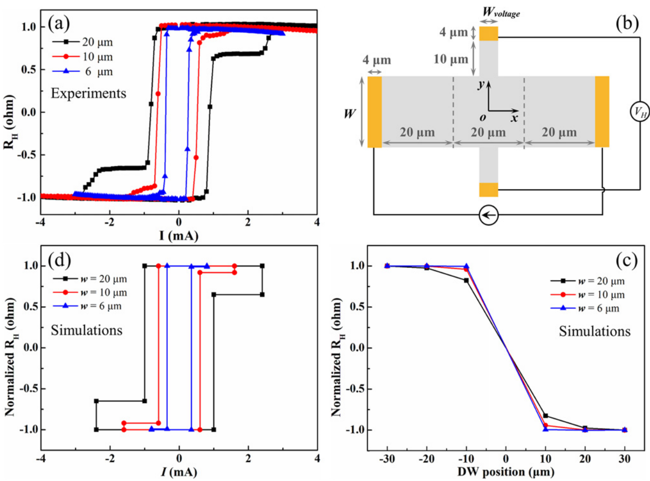

FIG. 4. (a) SOT-induced magnetization with $\mu_0 H_x = 50$ mT in irradiated Hall bars with different wire widths. (b) Schematic of the simulated cross-shaped Hall device. The normalized AHE resistance R_H as a function of (c) DW position and (d) SOT current.

changes, which indicates that R_H is dominated by the magnetization state of the irradiated region.[30,31] But the reduction of R_H with DW moving from $-30\,\mu$m to $-10\,\mu$m or from $10\,\mu$m to $30\,\mu$m also shows that the magnetization, which is out of the Hall cross, can be sensed by the Hall probes.[30,31] This effect becomes more prominent as w and $w_{voltage}$ increase. Specifically, the irradiated region contributes 99.5% to R_H when $w = 6\,\mu$m, but the contribution drops to 82.5% when $w = 20\,\mu$m. This is why the multi-level Hall resistance can only be evidenced in devices with $w = 20\,\mu$m. We also calculated the R_H change during the SOT switching in Fig. 3. Note that we assumed that there are only two critical SOT currents: I_{c1} for switching the magnetization in the irradiated region and I_{c2} for the switching of the rest of the magnetization. The value of the simulation currents is adopted from our experiments. As exhibited in Fig. 4(d), we can well reproduce the experimental results shown in Fig. 4(a), indicating that we can tailor the intermediate states through the design of device sizes (see the supplementary material) and the position of He^+ irradiation. Also note that although the individual switching of magnetization in the irradiated region cannot be sensed by Hall signals in devices with $w = 6\,\mu$m, it is evidenced by Kerr microscopy (see the supplementary material), suggesting the potential of He^+ ion irradiation to realize multi-state switching.

In summary, we demonstrated SOT-driven multi-level resistances in the W/CoFeB/MgO heterostructure working at low current density by inducing a lateral gradient of perpendicular magnetic anisotropy. The possibility to increase the number of intermediate states by designing different values of perpendicular anisotropy through He^+ ion irradiation paves the way toward power-efficient neuromorphic and memristor devices where the nucleation, motion, and pinning can be tailored.

See the supplementary material for the hysteresis loops under the in-plane magnetic field (S1), the finite element simulations of AHE (S2), the tailoring multi-level devices through device sizes (S3), and the magnetization reversal process in Hall bars with a width of $10\,\mu$m or $6\,\mu$m (S4).

AUTHORS' CONTRIBUTIONS

X.Z., Y.L., and D.Z. contributed equally to this work.

We gratefully acknowledge financial support from the National Key R&D Program of China (No. 2018YFB0407602), the European Union FP7 Program through contracts ITN WALL, Contract No. 608031, and the French National Research Agency though the projects COMAG and ELECSPIN. We also want to acknowledge funding from the project CNRS PREMAT "Spin- Ion."

DATA AVAILABILITY

The data that support the findings of this study are available from the corresponding author upon reasonable request.

REFERENCES

[1] L. Liu, C.-F. Pai, Y. Li, H. W. Tseng, D. C. Ralph, and R. A. Buhrman, Science **336**, 555 (2012).
[2] I. M. Miron, T. Moore, H. Szambolics, L. Daniela, B. Prejbeanu, S. Auffret, B. Rodmacq, S. Pizzini, J. Vogel, M. Bonfim, A. Schuhl, and G. Gaudin, Nat. Mater. **10**, 419 (2011).
[3] S. Fukami, C. L. Zhang, S. DuttaGupta, A. Kurenkov, and H. Ohno, Nat. Mater. **15**, 535 (2016).
[4] M. Wang, W. Cai, D. Zhu, Z. Wang, J. Kan, Z. Zhao, K. Cao, Z. Wang, Y. Zhang, T. Zhang, C. Park, J. Wang, A. Fert, and W. S. Zhao, Nat. Electron. **1**, 582 (2018).
[5] K. Garello, C. O. Avci, I. M. Miron, M. Baumgartner, A. Ghosh, S. Auffret, O. Boulle, G. Gaudin, and P. Gambardella, Appl. Phys. Lett. **105**, 212402 (2014).
[6] C. Zhang, S. Fukami, H. Sato, F. Matsukura, and H. Ohno, Appl. Phys. Lett. **107**, 012401 (2015).
[7] S. Zhang, Y. Su, X. Li, R. Li, W. Tian, J. Hong, and L. You, Appl. Phys. Lett. **114**, 042401 (2019).
[8] X. X. Zhao, X. Y. Zhang, H. W. Yang, W. L. Cai, Y. L. Zhao, Z. H. Wang, and W. S. Zhao, Nanotechnology **30**, 335707 (2019).
[9] S. Z. Peng, J. Q. Lu, W. X. Li, L. Z. Wang, H. Zhang, X. Li, K. L. Wang, and W. S. Zhao, in IEEE International Electron Devices Meeting (IEDM) (2019), p. 28.6.1.
[10] K. S. Ryu, L. Thomas, S.-H. Yang, and S. Parkin, Nat. Nanotechnol. **8**, 527 (2013).
[11] S. Emori, U. Bauer, S.-M. Ahn, E. Martinez, and G. S. D. Beach, Nat. Mater. **12**, 611 (2013).
[12] J. H. Franken, H. J. M. Swagten, and B. Koopmans, Nat. Nanotechnol. **7**, 499 (2012).
[13] M. Al Bahri, B. Borie, T. L. Jin, R. Sbiaa, M. Kläui, and S. N. Piramanayagam, Phys. Rev. Appl. **11**, 024023 (2019).
[14] R. Blasing, A. A. Khan, P. C. Filippou, C. Garg, F. Hameed, J. Castrillon, and S. Parkin, "Magnetic racetrack memory: From physics to the cusp of applications within a decade," Proc. IEEE (published on line, 2020).
[15] S. Zhang, S. J. Luo, N. Xu, Q. M. Zou, M. Song, J. J. Yun, Q. Luo, Z. Guo, R. F. Li, W. C. Tian, X. Li, H. G. Zhou, H. M. Chen, Y. Zhang, X. F. Yang, W. J. Jiang, K. Shen, J. M. Hong, Z. Yuan, L. Xi, K. Xia, S. Salahuddin, B. Dieny, and L. You, Adv. Electron. Mater. **5**, 1970022 (2019).
[16] J. R. Whyte, R. G. P. McQuaid, C. M. Ashcroft, J. F. Einsle, C. Canalias, A. Gruverman, and J. M. Gregg, J. Appl. Phys. **116**, 066813 (2014).
[17] S. Lequeux, J. Sampaio, V. Cros, K. Yakushiji, A. Fukushima, R. Matsumoto, H. Kubota, S. Yuasa, and J. Grollier, Sci. Rep. **6**, 31510 (2016).
[18] X. X. Zhao, B. Y. Zhang, N. Vernier, X. Y. Zhang, M. Sall, T. Xing, L. H. Diez, C. Hepburn, L. Wang, G. Durin, A. Casiraghi, M. Belmeguenai, Y. Roussigné, A. Stashkevich, S. M. Chérif, J. Langer, B. Ocker, S. Jaiswal, G. Jakob, M. Kläui, W. S. Zhao, and D. Ravelosona, Appl. Phys. Lett. **115**, 122404 (2019).
[19] L. H. Diez, M. Voto, A. Casiraghi, M. Belmeguenai, Y. Roussigné, G. Durin, A. Lamperti, R. Mantovan, V. Sluka, V. Jeudy, Y. T. Liu, A.

Published under license by AIP Publishing

Stashkevich, S. M. Chérif, J. Langer, B. Ocker, L. Lopez-Diaz, and D. Ravelosona, Phys. Rev. B **99**, 054431 (2019).
[20]D. A. Gilbert, B. B. Maranville, A. L. Balk, B. J. Kirby, P. Fischer, D. T. Pierce, J. Unguris, J. A. Borchers, and K. Liu, Nat. Commun. **6**, 8462 (2015).
[21]P. K. Greene, J. Osten, K. Lenz, J. Fassbender, C. Jenkins, E. Arenholz, T. Endo, N. Iwata, and K. Liu, Appl. Phys. Lett. **105**, 072401 (2014).
[22]T. Devolder, J. Ferré, C. Chappert, H. Bernas, J. P. Jamet, and V. Mathet, Phys. Rev. B **64**, 064415 (2001).
[23]Y. Zhang, X. Y. Zhang, N. Vernier, Z. Z. Zhang, G. Agnus, J.-R. Coudevylle, X. Y. Lin, Y. Zhang, Y. G. Zhang, W. S. Zhao, and D. Ravelosona, Phys. Rev. Appl. **9**, 064027 (2018).
[24]J. H. Franken, M. Hoeijmakers, R. Lavrijsen, J. T. Kohlhepp, H. J. M. Swagten, B. Koopmans, E. Van Veldhoven, and D. J. Maas, J. Appl. Phys. **109**, 07D504 (2011).
[25]R. L. Conte, E. Martinez, A. Hrabec, A. Lamperti, T. Schulz, L. Nasi, L. Lazzarini, R. Mantovan, F. Maccherozzi, S. S. Dhesi, B. Ocker, C. H. Marrows, T. A. Moore, and M. Kläui, Phys. Rev. B **91**, 014433 (2015).
[26]L. Zhang, X. Zhang, M. Wang, Z. Wang, W. Cai, K. Cao, D. Zhu, H. Yang, and W. S. Zhao, Appl. Phys. Lett. **112**, 142410 (2018).
[27]J. Sinova, S. O. Valenzuela, J. Wunderlich, C. H. Back, and T. Jungwirth, Rev. Mod. Phys. **87**, 1213 (2015).
[28]A. Kirilyuka, J. Ferréa, V. Groliera, J. P. Jameta, and D. Renard, J. Magn. Magn. Mater. **171**, 45 (1997).
[29]J. Sun and J. Kosel, *Finite Element Analysis–New Trends and Developments* (ExLi4EvA, 2016), Chap. 10.
[30]A. Thiaville, L. Belliard, D. Majer, E. Zeldov, and J. Miltat, J. Appl. Phys. **82**, 3182 (1997).
[31]J. Wunderlich, Ph.D. thesis, University of Paris-Sud, 2001.

Published under license by AIP Publishing